Bulletin of the Geological Survey of Japan, vol. 71 (1), p. 33–48, 2020

Report

LA–ICP–MS zircon U–Pb ages of felsic tuffaceous beds in the Takikubo and Horita formations, Izumi Group, Ikeda district, eastern Shikoku, southwestern Japan

NODA Atsushi[1,*], DANHARA Tohru[2], IWANO Hideki[2] and HIRATA Takafumi[3]

Noda Atsushi, Danhara Tohru, Iwano Hideki and Hirata Takafumi (2020) LA-ICP-MS U–Pb ages of felsic tuffaceous beds in the Takikubo and Horita formations, Izumi Group, Ikeda district, eastern Shikoku, southwestern Japan. *Bulletin of the Geological Survey of Japan*, vol. 71 (1), p. 33–48, 7 figs, 5 tables.

Abstract: Laser ablation–inductively coupled plasma–mass spectrometry zircon U–Pb ages were acquired for three felsic tuffaceous beds, one from the upper Takikubo Formation (sample IT01) and two from the lower Horita Formation (IT02 and IT03), to determine depositional ages of the Izumi Group in the Ikeda district, eastern Shikoku, southwestern Japan. The weighted mean $^{206}Pb/^{238}U$ ages and 2σ errors are 78.3 ± 1.3 Ma (IT01), 80.8 ± 1.2 Ma (IT02), and 79.3 ± 1.1 Ma (IT03). Two of the three ages (78.3 ± 1.3 Ma and 79.3 ± 1.1 Ma) passed the χ^2_{red} (reduced) statistical test, but the other (80.8 ± 1.2 Ma) failed. These U–Pb ages indicate that the maximum depositional age of the Izumi Group in this district is middle Campanian (magnetostratigraphic chron C33n). These ages are similar to those reported from the lower Takikubo Formation in the Kan-onji district (80.8–78.3 Ma). Although an apparent stratigraphic thickness from the lower Takikubo Formation to the lower Horita Formation reaches 12 km, there is no younging trend of the zircon U–Pb ages through these formations. This suggests that either the sedimentation rate of the Izumi Group was high or there was a lack of volcanic activity that could produce new zircon crystals in the hinterland during deposition of the succession.

Keywords: Campanian, Cretaceous, Felsic tuff, Izumi Group, Shikoku, Takikubo Formation, Horita Formation, U–Pb age, Zircon

1. Introduction

The Izumi Group (Matsumoto, 1954) consists of shallow- to deep-marine deposits that are distributed in a 10–20-km-wide and 300-km-long zone along the northern side of the Median Tectonic Line, from western Shikoku to the Kii Peninsula, southwestern Japan (Fig. 1). Paleontological evidence, including macro-fossils (ammonoids and inoceramids) and micro-fossils (radiolarian assemblages), indicates that the depositional age of the Izumi Group is Campanian–Maastrichtian (Late Cretaceous) and that it youngs toward the east (Suyari, 1973; Bando and Hashimoto, 1984; Yamasaki, 1987; Hashimoto *et al.*, 2015). Although a few studies have reported occurrences of macrofossils from the Izumi Group in the Ikeda district, eastern Shikoku, their age resolution is inadequate to discuss details of the depositional ages of the Izumi Group. In addition, radiometric age data from the Izumi Group in eastern Shikoku are sparse; until now, only two ages have been reported from eastern Shikoku (Noda *et al.*, 2017b). Therefore, further radiometric age data were required to constrain detailed depositional ages and the sedimentation rate of the strata. This paper reports new laser ablation–inductively coupled plasma–mass spectrometry (LA–ICP–MS) U–Pb ages of detrital zircons in felsic tuff beds, including one sample from the Takikubo Formation and two samples from the Horita Formation of the Izumi Group, in the Ikeda district, eastern Shikoku.

2. Geological background

The Izumi Group in eastern Shikoku is composed of a main facies and a northern marginal facies (Matsuura *et al.*, 2002). The main facies comprises alternating beds of sandstone and mudstone and is divided into four formations: the Takikubo, Horita, Higaidani, and Bandodani formations, from the lowermost (west) to uppermost (east) (Yamasaki, 1986). The northern marginal facies consists of two formations: the Shiroyama Formation (conglomerate and sandstone) and the Hiketa Formation (massive mudstone).

[1] AIST, Geological Survey of Japan, Research Institute of Geology and Geoinformation
[2] Kyoto Fission-Track Co., Ltd., 44-4 Minamitajin-cho, Omiya, Kita-ku, Kyoto 603-8832. Japan
[3] Geochemical Research Center, Graduate School of Science, The University of Tokyo, 7-3-1 Hongo, Bunkyo-ku, Tokyo 113-0033, Japan
[*] Corresponding author: NODA, A., Central 7,1-1-1 Higashi, Tsukuba, Ibaraki 305-8567, Japan. Email:a.noda@aist.go.jp

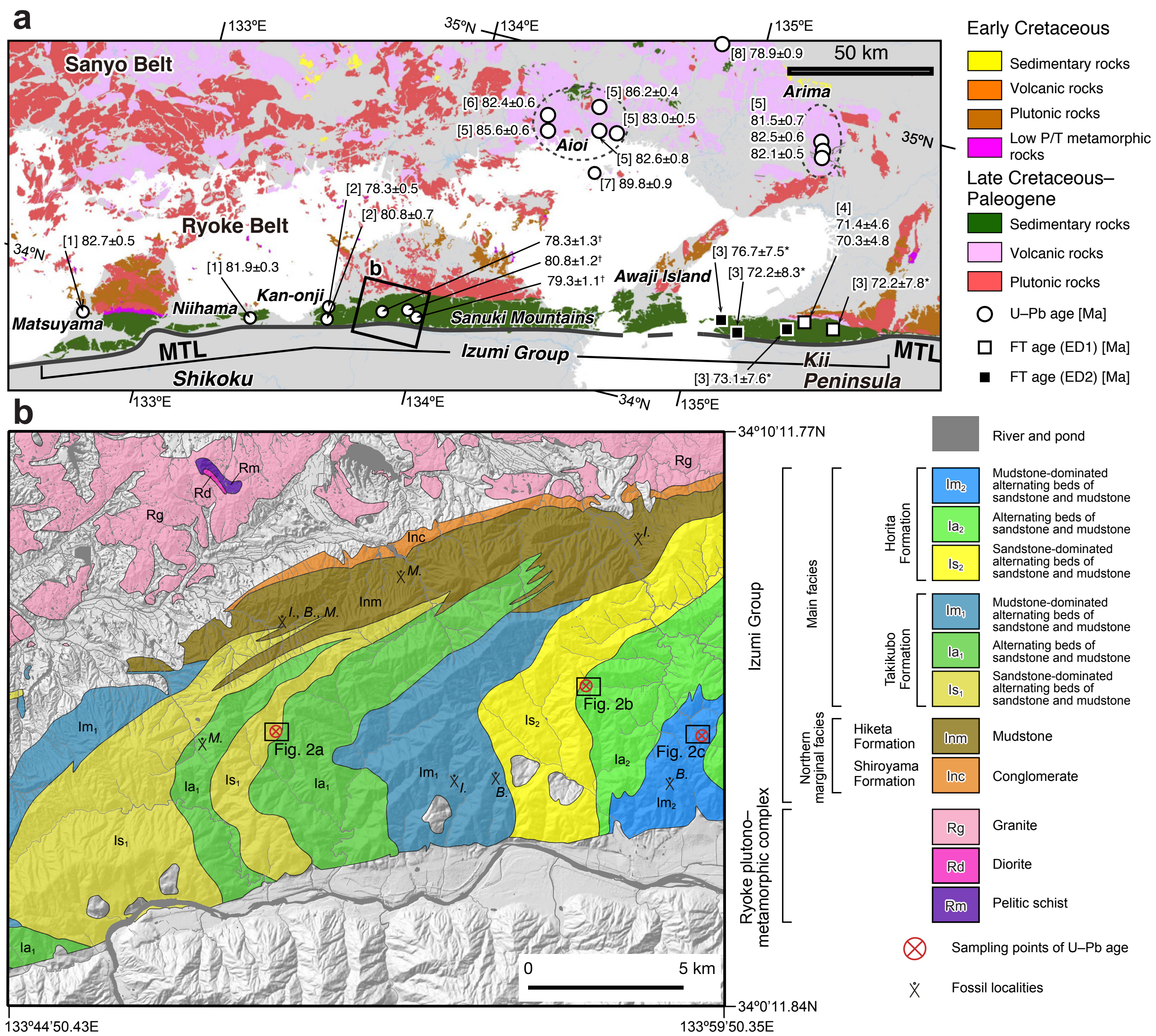

Fig. 1 (a) Overview map showing the locations of previously reported U–Pb and fission-track (FT) ages (2σ). FT ages include data obtained using the external-detector method using internal surfaces (ED1) and external surfaces (ED2). The geological map is reproduced from the Seamless Digital Geological Map of Japan (Geological Survey of Japan, AIST, 2015). The inclined square shows the Ikeda district. MTL = Median Tectonic Line. References: [1] Noda and Sato (2018), [2] Noda *et al.* (2017b), [3] Miyata (2004), [4] Seike *et al.* (2013), [5] Sato *et al.* (2016b), [6] Sato *et al.* (2016a), [7] Sato (2016), and [8] Sato (2015). Asterisks (*) denote FT ages recalculated from the original data using a decay constant of $D = 1.55125 \times 10^{-10}\,\mathrm{yr}^{-1}$ instead of $1.480 \times 10^{-10}\,\mathrm{yr}^{-1}$. Daggers (†) indicate U–Pb ages from this study. Modified from Noda and Sato (2018). (b) Locations of felsic tuff samples collected for U–Pb age determinations. The geological map is from the Geological Survey of Japan, AIST (2015). The shaded topography is based on GSI Maps (http://maps.gsi.go.jp/). Abbreviations of fossil localities: *M.*, *Metaplacenticeras subtilistriatum*; *B.*, *Baculites* sp.; *I.*, *Inoceramus balticus*.

A series of studies in the 1960s and 1970s identified the following features of the Izumi Group: (1) the strata young from west to east; (2) the paleocurrent directions in the main facies are largely from east to west, opposite to the younging direction; and (3) the northern marginal facies interfingers the main facies (Suyari, 1966; Suyari *et al.*, 1968; Suyari, 1973).

The Ikeda district contains the lower two formations of the main facies, the Takikubo and Horita formations, and the northern marginal facies, the Shiroyama and Hiketa formations (Fig. 1). Both the Takikubo and the Horita formations are dominated by alternating beds of sandstone and mudstone, but the proportion of sandstone to mudstone changes within the formation. The lower part of the Takikubo Formation in the Kan-onji district, which is situated at the west of the Ikeda district, is subdivided

Table 1 A list of analyzed samples. Longitude and latitude are given in the WGS84 datum.

Sample no.	ID	Longitude	Latitude	Date	Loc no.	Lithology	GSJ reg. no.
IT01	2469	133°50'26.9"E	34°4'58.8"N	2016-11-11	01	Felsic tuffaceous sandstone	R109880
IT02	6326	133°56'56.4"E	34°5'46.3"N	2017-12-09	02	Felsic tuff	R109881
IT03	2368	133°59'21.8"E	34°4'54.1"N	2016-11-10	03	Felsic tuffaceous sandstone	R109882

into the Minoura Sandstone and Mudstone Member, Tanono Sandstone Member, Ebisukui Mudstone Member, and Umpenji Sandstone Member as the stratigraphic order based on the dominant lithology (Noda *et al.*, 2017a). However, upper part of the Takikubo and the Horita formations have not yet been subdivided into members.

The depositional environments for the Izumi Group are thought to have been a line-sourced slope or fan delta in the marginal facies and a point-sourced submarine fan in the main facies (Nishiura *et al.*, 1993; Tanaka, 1993; Tanaka and Maejima, 1995; Noda and Toshimitsu, 2009). Sandstone in the Izumi Group is mostly lithic, although some is quartzo-feldspathic (Nishimura, 1976). The chemical compositions of heavy minerals (garnet and spinel) in the sandstone indicate that their source was the granitic and metamorphic rocks exposed in the Ryoke and Sanyo belts (Yokoyama and Goto, 2000).

Yamasaki (1987) and Hashimoto *et al.* (2015) identified several radiolarian fossil zones in the Izumi Group, and the upper Takikubo Formation together with the Horita Formation correspond to the *Archaeodictyomitra lamellicostata* Zone. Several macro-fossils have been reported in this district (Fig. 1), and ammonite fossils characterized by *Metaplacenticeras subtilistriatum* have been found in the adjacent Hiketa Formation (Bando and Hashimoto, 1984). A few occurrences of *Baculites* sp. have been recognized in the upper Takikubo Formation (Ishida *et al.*, 1993) and the lower Horita Formation (Hashimoto *et al.*, 2003). Some occurrences of *Inoceramus balticus* are also reported in the Hiketa Formation and the upper Takikubo Formation (Nakano, 1953; Bando and Hashimoto, 1984). These fossils indicate that the Izumi Group in this district is the lower part of the upper Campanian.

3. Samples and methods

3.1 Samples

One sample (IT01) from the upper Takikubo Formation and two samples (IT02 and IT03) from the lower Horita Formation were collected from the Ikeda district, in the central Sanuki Mountains, eastern Shikoku (Fig. 1 and Table 1).

The sampling locality of IT01 is situated within the sandstone-dominated sequence of the Umpenji Sandstone Member (Noda *et al.*, 2017a) of the Takikubo Formation (Fig. 2a). IT01 was collected from a medium-bedded fine- to medium-grained light-gray felsic tuffaceous sandstone (Fig. 3a). The tuffaceous sandstone constitutes a 3-m-thick tuffaceous unit. The sandstone shows weak parallel laminations, and flattened pumice clasts (<6 mm in length) and plagioclase crystals (<1 mm in length) are common. Under the microscope, it is classified as a vitric–crystal tuff containing flattened glass shards (pumice) and quartz and plagioclase crystals (Fig. 3b). The matrix has a felsitic texture.

IT02 was collected from a felsic tuff bed in the basal sandstone-dominated succession of the Horita Formation (Fig. 2b). The total thickness of the felsic tuff bed is <20 m, and it is composed of medium- to thickly bedded felsic tuff (Fig. 3c). The sample is a light-gray fine-grained medium-bedded vitric tuff with parallel laminations. Bubble-wall glass shards dominate, with a few crystals and lithic fragments being observed under the microscope (Fig. 3d).

IT03 was collected from a fine-grained, thick-bedded tuffaceous sandstone which was intercalated within the mudstone-dominated facies of the Horita Formation (Fig. 2c). The tuffaceous sandstones constitute more than 30-m-thick tuffaceous unit with thinly to medium-bedded dark-gray mudstone (Fig. 3e). The sample is a vitric–crystal–lithic tuff containing embayed quartz and felsic volcanic rock fragments with bubble-wall glass shards (Fig. 3f).

3.2 Methods

Zircon grains were separated from the samples by crushing, sieving, panning, magnetic, and heavy liquid (sodium polytungstate) techniques, and then mounted on a PFA Teflon sheet. U–Pb dating was performed using the LA–ICP–MS system installed in the Geochemical Research Center, Graduate School of Science, The University of Tokyo, Japan. The LA–ICP–MS system consisted of an ICP–MS instrument (iCAP Qc, Thermo Fisher Scientific, Waltham, MA, USA) and a femtosecond LA instrument (IFRIT Type-C, Cyber Laser Inc., Tokyo, Japan). The operating conditions for the LA and ICP–MS instruments are summarized in Table 2. The laser had a wavelength of 260 nm, an energy of 2–3 J/cm^2, a spot size of 15 µm (IT01 and IT03) or 10 µm (IT02), and a repetition rate of 15 Hz (IT01 and IT03) or 10 Hz (IT02). Helium was used as the carrier gas inside the ablation cell and was mixed with argon before entering the ICP–MS. Signal intensities for ^{202}Hg, ^{204}(Pb + Hg), ^{206}Pb, ^{207}Pb, ^{208}Pb, ^{232}Th, and ^{238}U were obtained from 30 zircon crystals in each sample.

The contribution of common Pb was monitored using the ^{204}Pb signal with ^{204}Hg as an isobaric interference. The

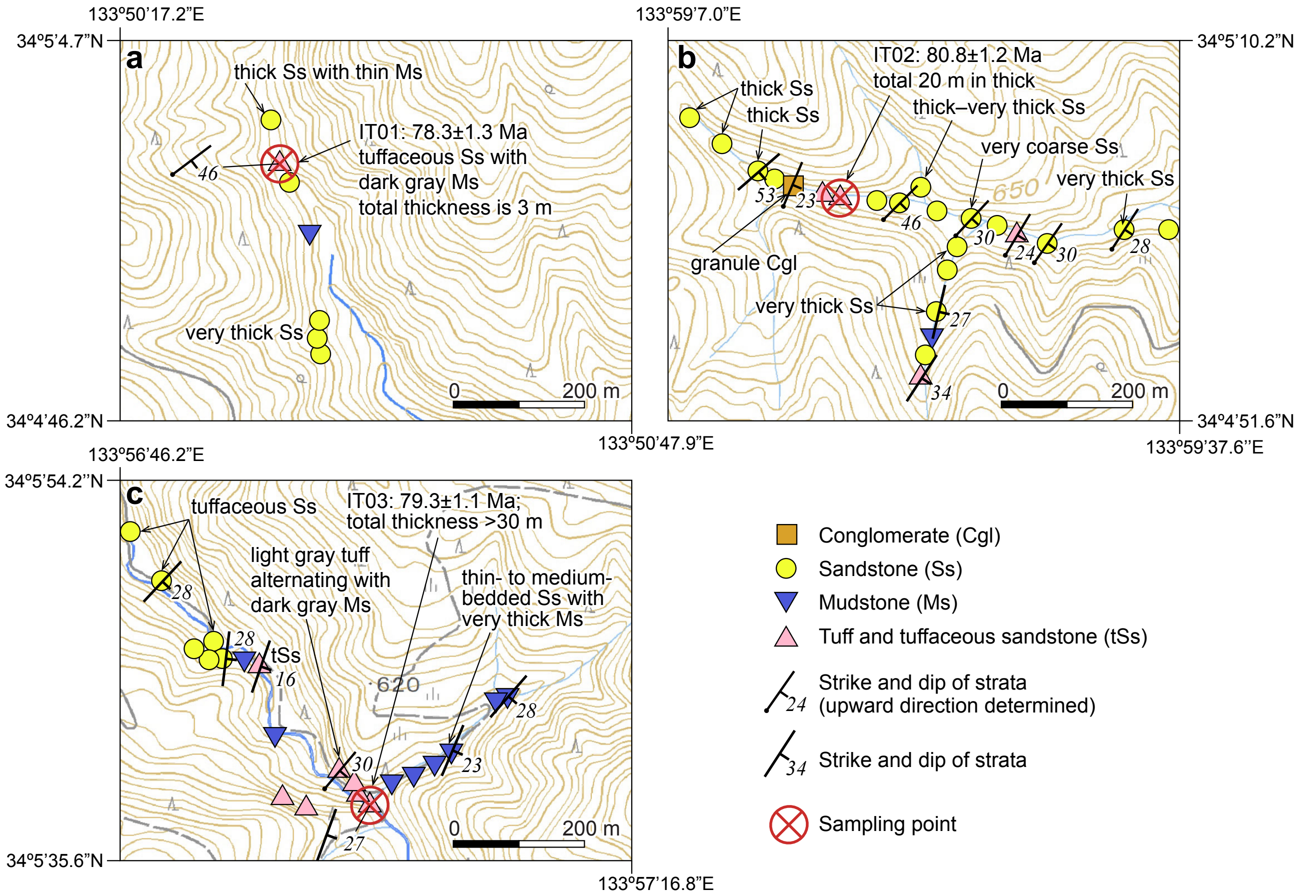

Fig. 2 Locations of sampling points of (a) IT01, (b) IT02, and (c) IT03. The topographic maps are based on GSI Maps (http://maps.gsi.go.jp/).

abundance of ^{204}Hg was calculated from blank-corrected ^{202}Hg on the basis of the natural ^{202}Hg/^{204}Hg ratio, which in turn was subtracted from the total 204 signal to yield ^{204}Pb. We applied one-shot cleaning on the sample surfaces before the analysis to reduce the risk of common-Pb contamination. Instrumental bias in the ^{206}Pb*/^{238}U ratio (asterisk denotes radiogenic) was corrected using 91500 zircon (Wiedenbeck *et al.*, 1995) as a primary standard, and OD-3 (Iwano *et al.*, 2012, 2013), GJ-1(Jackson *et al.*, 2004), and Plešovice (Sláma *et al.*, 2008) zircons as secondary standards (Tables 3–5).

The resultant U–Pb isotopic ratios and errors were used to plot concordia diagrams and histograms using UPbplot.py version 0.0.9 (Noda, 2017). The latest version of this software can be downloaded from the website (https://github.com/anoda/UPbplot.py). Discordance was calculated using the following equation:

$$\text{Discordance} = \left(1 - \frac{^{206}\text{Pb}^{*}/^{238}\text{U age}}{^{207}\text{Pb}^{*}/^{235}\text{U age}}\right) \times 100$$

We excluded data whose discordance exceeded 20 % from the age calculations. We then applied the generalized ESD (extreme Studentized deviate) test to exclude outliers (Rosner, 1983). Details of this test are described in the Appendix. We also calculated reduced chi-squared statistics (χ^2_{red}; Spencer *et al.*, 2016). If χ^2_{red} for the uncertainties and weighted mean of the observed data do not fall inside of the range of $1 \pm 2\sqrt{2/f}$, where f is the degrees of freedom ($n-1$), the hypothesis that the weighted mean represents the depositional age of the observed data set is rejected with a probability of >95 %. χ^2_{red} is equivalent to the mean square weighted deviation (MSWD; Wendt and Carl, 1991). For the case of $\chi^2_{\text{red}} > 1 + 2\sqrt{2/f}$, the assumed analytical errors of the measurement are too small, or the data are not sampled from a single statistical population, that is, there is a mixing of multiple populations. In contrast, $\chi^2_{\text{red}} < 1 - 2\sqrt{2/f}$ indicates that the grains could be derived from a single population but the analytical uncertainties are overestimated.

4. Results

We analyzed 30 zircon grains in each sample. The ^{206}Pb/^{238}U, ^{207}Pb/^{235}U, and ^{207}Pb/^{206}Pb ages of zircons were calculated using the measured isotopic ratios and decay constants.

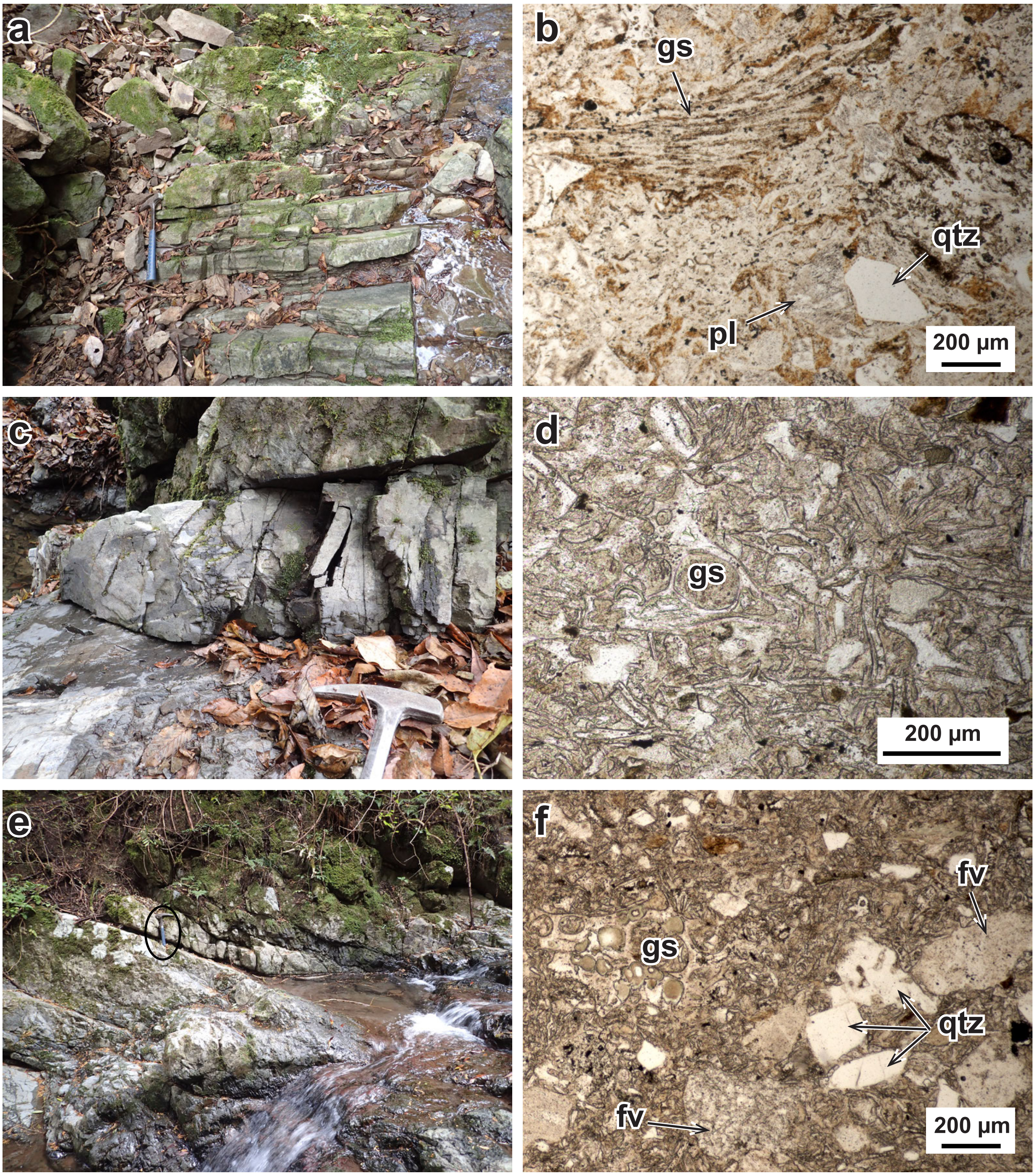

Fig. 3 (a) Photograph of an outcrop of the felsic tuff bed from which sample IT01 was obtained, showing a 3-m-thick tuff bed containing repetitions of thin- to medium-bedded tuff. The hammer is 33 cm in length. Munegi, Higashiyama, Higashimiyoshi Town, Miyoshi County, Tokushima Prefecture. (b) Photomicrograph of IT01 (plane-polarized light). (c) Photograph of the outcrop from which sample IT02 was obtained. The hammer head is 18 cm long. Shimobuke, Katsuura, Manno Town, Nakatado County, Kagawa Prefecture. (d) Photomicrograph of IT02 (plane-polarized light). Fragments of glass shards dominate. (e) Photograph of the outcrop from which sample IT03 was obtained. A circle indicates location of a hammer as a scale, whose length is 33 cm. Hachimine, Katsuura, Manno Town, Nakatado County, Kagawa Prefecture. (f) Photomicrograph of IT03 (plane-polarized light). Abbreviations: gs, glass shards; qtz, quartz; pl, plagioclase; fv, felsic volcanic rock fragments.

Table 2 ICP–MS and laser operating conditions and data acquisition parameters.

Parameters	Value/Description
Laser ablation	
Model	IFRIT (Cyber Laser Inc., Tokyo, Japan)
Laser type	Type-C Ti:S femtosecond laser
Laser wave length	260 nm (THG)
Laser energy	2–3 J/cm^2
Pulse width	230 fs
Ablation crater size	10 μm (IT02) 15 μm (IT01 & IT03)
Repetition rate	10 Hz (IT02) 20 Hz (IT01 & IT03)
Carrier gas (flow rate)	He (0.60–0.83 L/min)
ICP-MS	
Model	iCAP-Qc (Thermo Fisher Scientific, Waltham, MA, USA)
ICP-MS type	Quadrupole
Forward power	1400 W
Carrier gas (flow rate)	Ar (0.90–1.10 L/min)
Scanning mode	Standard mode
Data acquisition protocol	50 s (15 s gas blank, 35 s ablation)
Analysis mode	Time-resolved analysis
Monitor isotopes	^{202}Hg, ^{204}(Hg + Pb), ^{206}Pb, ^{207}Pb, ^{208}Pb, ^{232}Th, ^{238}U
Dwell time	0.2 s for $^{206, 207, 208}$Pb, 0.1 s for others
Standard materials	
91500	Wiedenbeck *et al*. (1995)
OD-3	Iwano *et al*. (2012), Iwano *et al*. (2013), Lukács *et al*. (2015)
GJ-1	Jackson *et al*. (2004)
Plěsovice	Sláma *et al*. (2008)

4.1 Sample IT01

This sample contained abundant fine- to medium-sized euhedral zircon grains. Approximately 1,000 grains were extracted from 300 g of the sample. A total of 26 concordant analyses form a nearly unimodal distribution clustered between 82 and 73 Ma (Fig. 4; Table 3), with three older ages around 96–90 Ma. The generalized ESD test eliminated these older ages as outliers, and 23 grains were therefore accepted for age calculation. The conventional concordia (^{207}Pb/^{235}U–^{206}Pb/^{238}U), Tera–Wasserburg concordia (^{238}U/^{206}Pb–^{207}Pb/^{206}Pb), and weighted mean ^{206}Pb/^{238}U ages and 2σ errors are 78.3 ± 1.3 Ma, 78.5 ± 1.3 Ma, and 78.3 ± 1.3 Ma, respectively (Fig. 4). The weighted mean ^{206}Pb/^{238}U age and uncertainties passed the reduced chi-squared test (χ^2_{red} = 0.5). High Th/U ratios (0.35–1.00) indicate that the zircon grains are igneous in origin (e.g., Hoskin and Schaltegger, 2003).

4.2 Sample IT02

Zircon grains in this sample are mostly fine grained and euhedral to subhedral. About 200 zircons were separated from 300 g of this sample, fewer than from the other samples. Owing to the relatively large analytical errors, 10 of the 30 analyses were discordant (Fig. 5; Table 4). The single-grain ages from IT02 are widely spread, ranging from 73 to 90 Ma. The generalized ESD test did not exclude any of the 20 concordant analyses. The accepted data (n = 20) yield a conventional concordia age of 80.6 ± 1.1 Ma (2σ), a Tera–Wasserburg concordia age of 81.2 ± 1.1 Ma, and a weighted mean ^{206}Pb/^{238}U age of 80.8 ± 1.2 Ma (Fig. 5c). The χ^2_{red} test for the weighted mean of ^{206}Pb/^{238}U ages failed ($\chi^2_{red} > 1 \pm 2\sqrt{2/f}$). The Th/U ratios (0.37–0.85) are similar to those of IT01 and similarly indicate an igneous origin.

4.3 Sample IT03

IT03 contains abundant zircons, and about 10,000 grains were obtained from 300 g of the sample. The zircon crystals are mainly fine to medium grained and show euhedral prismatic shapes. A total of 28 concordant analyses form a single peak around 78 Ma, with several older analyses from 240 to 80 Ma (Fig. 6; Table 5). We removed six data points from the age calculations based on the generalized ESD test, leaving 22 analyses. The resultant conventional concordia, Tera–Wasserburg concordia, and weighted mean ^{206}Pb/^{238}U ages are 79.3 ± 1.0 Ma, 79.6 ± 1.0 Ma, and 79.3 ± 1.1 Ma, respectively. The weighted mean ^{206}Pb/^{238}U age passed the χ^2_{red} test (χ^2_{red}= 1.3; n = 22). The range of Th/U ratios (0.42–0.90) is similar to those of the other samples.

5. Discussion

Samples IT01 and IT03 show unimodal age distributions and pass the χ^2_{red} test, indicating that their ^{206}Pb/^{238}U ages form single statistical populations. These ages (78.3 ± 1.3 Ma for IT01 and 79.3 ± 1.1 Ma for IT03) can be considered to be the maximum depositional ages of the tuff beds from which the samples were taken, and they correspond to the middle Campanian and polarity chron C33n (Ogg *et al.*, 2012). However, the U–Pb ages of sample IT02 are widely spread on a histogram and fail the χ^2_{red} test. This suggests that the IT02 data could be a mixture of multiple populations or that the analytical uncertainties were underestimated.

One reason that IT02 contains more discordant data (n = 10) is likely to be the relatively low analytical precision, especially that of ^{207}Pb, possibly because of the smaller size of the zircon crystals and the ablation crator size compared with the other samples (Table 2). Lead loss caused by post-depositional regional metamorphism is considered unlikely, as the concordia plots do not indicate stoichiometric loss of ^{207}Pb/^{206}Pb, and only sample IT02 contains a substantial number of discordant analyses. However, zircon grains might have lost Pb during pre-

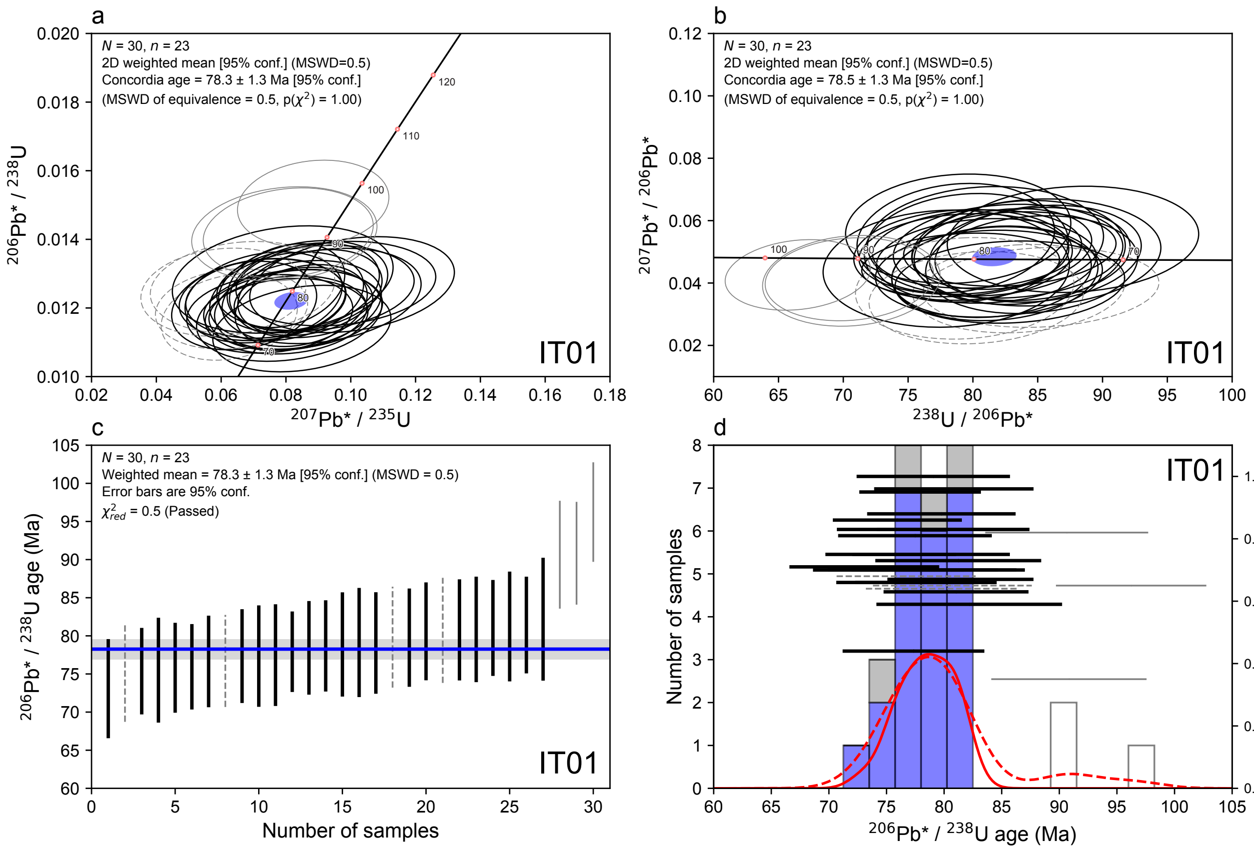

Fig.4 U–Pb dating results for IT01. (a) $^{207}Pb^{*}/^{235}U$–$^{206}Pb^{*}/^{238}U$ concordia diagram (Wetherill, 1956). Asterisks (*) of $^{206}Pb^{*}$ and $^{207}Pb^{*}$ denote radiogenic. Solid black, solid gray, and dashed gray ellipses represent 2σ errors of accepted, excluded, and discordant data points, respectively. The blue ellipse is the 95 % confidence region of the two-dimensional weighted mean. N and n are numbers of total and accepted grains, respectively. Data exclusion was based on the generalized ESD test (Rosner, 1983) for the weighted mean $^{206}Pb/^{238}U$ age and 2σ uncertainties. (b) Tera–Wasserburg concordia diagram (Tera and Wasserburg, 1972). The description is the same as for (a). (c) One-dimensional weighted mean $^{206}Pb/^{238}U$ age (blue line) and its 2σ error (gray band). Solid black, solid gray, and dashed gray lines represent accepted, excluded, and discordant data (2σ), respectively. (d) Th/U ratios (right-hand axis with horizontal black and gray lines) and stacked $^{206}Pb/^{238}U$ age histograms (left-hand vertical axis), with accepted (blue bars), excluded (white bars), and discordant (gray bars) data. Solid red and dashed red lines represent (kernel density estimation) for accepted (n = 23) and all (n = 30) data.

depositional metasomatism in the source area. Local fluid alteration in glassy tuff beds is also a possible cause of Pb loss, although there is no evidence of intrusive rocks or hydrothermal alteration around the sampling site.

The ages obtained during this study are similar to previously reported ages from the lower Takikubo Formation (78.3 ± 0.5 Ma for KT01 and 80.8 ± 0.7 Ma for KT02, Noda *et al.*, 2017b). The age of KT02 may not be reliable, as the data show multiple peaks on a histogram, and the χ^2_{red} statistic (3.9; n = 7) shows that the data are widely dispersed. Therefore, the maximum depositional ages of the Takikubo and Horita formations range between 79.3 ± 1.1 and 78.3 ± 1.3 Ma, based on three accepted samples (KT01, IT01, and IT03; Fig. 7). The U–Pb ages obtained from the Takikubo and the Horita formations show no younging trend according to the stratigraphic position (Fig. 7).

There are three possible interpretations can be regarded for the similar zircon U–Pb ages obtained from the different stratigraphic positions, which include (1) a repetition of the same stratigraphic unit by faults, (2) a rapid sedimentation, and (3) an intermittent volcanic activity. As for the first interpretation, an interfingering relationship between the northern marginal facies and the main facies (Fig. 1) indicates that stratigraphically upper sequences progressively deposited eastward, and no large-scale faults can be recognized to stack the same stratigraphic units repeatedly (Matsuura *et al.*, 2002; Noda *et al.*, 2017a). In addition, there is a difference in occurrences of tuff beds in each formation; for example, the upper part of the Takikubo Formation (the Umpenji Sandstone Member) contains fewer tuff beds than the lower part of the Horita Formation (Matsuura *et al.*, 2002; Noda *et al.*, 2017a). This suggests that both formations

Table 3 U–Pb data from IT01. Daggers (†) and double daggers (‡) denote discordant data and data excluded from the calculation of concordia and weighted mean ages, respectively. Asterisks (*) of $^{206}Pb^*$ and $^{207}Pb^*$ denote radiogenic.

Sample IT01	Total count						Isotopic ratio						Disc.	Age [Ma]			
Grain#	^{206}Pb	^{207}Pb	^{232}Th	^{235}U	^{238}U	Th/U	$^{207}Pb^*/^{206}Pb^*$	2σ	$^{206}Pb^*/^{238}U$	2σ	$^{207}Pb^*/^{235}U$	2σ	[%]	$^{206}Pb^*/^{238}U$	2σ	$^{207}Pb^*/^{235}U$	2σ
1 ‡	1970	86	28227	808	111388	0.35	0.0412	0.0107	0.01419	0.001053	0.0807	0.0211	concordant	90.8	6.8	78.8	21.2
2	1546	89	46818	707	97548	0.67	0.0544	0.0141	0.01271	0.000990	0.0954	0.0248	concordant	81.4	6.4	92.5	24.9
3	1513	69	46897	719	99172	0.66	0.0431	0.0122	0.01224	0.000958	0.0728	0.0207	concordant	78.4	6.2	71.4	20.8
4 ‡	1535	66	50699	631	86960	0.82	0.0407	0.0117	0.01416	0.001105	0.0795	0.0230	concordant	90.6	7.1	77.6	23.1
5 †	1182	44	34532	552	76095	0.64	0.0353	0.0119	0.01246	0.001033	0.0607	0.0205	–33.4	79.8	6.7	59.8	20.7
6 †	1057	43	31155	488	67265	0.65	0.0383	0.0131	0.01260	0.001076	0.0666	0.0229	–23.3	80.7	6.9	65.5	23.0
7 ‡	3506	159	86832	1356	186959	0.65	0.0426	0.0091	0.01504	0.001020	0.0884	0.0188	concordant	96.3	6.6	86.0	18.9
8	1822	96	66703	902	124306	0.75	0.0494	0.0125	0.01176	0.000885	0.0802	0.0202	concordant	75.4	5.7	78.3	20.3
9	1504	80	47822	732	100890	0.66	0.0498	0.0134	0.01196	0.000937	0.0822	0.0222	concordant	76.6	6.0	80.3	22.3
10 †	1476	60	48146	718	98945	0.68	0.0382	0.0114	0.01197	0.000942	0.0632	0.0189	–23.3	76.7	6.1	62.2	19.0
11	3518	190	156966	1684	232128	0.95	0.0509	0.0104	0.01216	0.000824	0.0854	0.0172	concordant	77.9	5.3	83.2	17.3
12	2024	106	83932	994	137002	0.86	0.0493	0.0120	0.01185	0.000874	0.0806	0.0196	concordant	75.9	5.6	78.7	19.7
13	1399	76	44565	647	89215	0.70	0.0513	0.0140	0.01258	0.001002	0.0891	0.0245	concordant	80.6	6.5	86.7	24.6
14	1731	80	56229	821	113137	0.70	0.0435	0.0117	0.01228	0.000934	0.0737	0.0198	concordant	78.7	6.0	72.2	19.9
15	1556	76	52929	765	105511	0.70	0.0459	0.0126	0.01183	0.000920	0.0750	0.0206	concordant	75.8	5.9	73.5	20.7
16	2380	119	87218	1094	150779	0.83	0.0493	0.0104	0.01261	0.001035	0.0857	0.0186	concordant	80.8	6.7	83.5	18.8
17	4045	188	112874	1853	255476	0.63	0.0458	0.0082	0.01265	0.000982	0.0800	0.0146	concordant	81.0	6.3	78.2	14.7
18	885	40	22924	400	55148	0.59	0.0446	0.0151	0.01283	0.001258	0.0790	0.0274	concordant	82.2	8.1	77.2	27.4
19	1769	88	75386	812	112008	0.96	0.0490	0.0117	0.01262	0.001080	0.0853	0.0210	concordant	80.8	7.0	83.1	21.1
20	1290	70	40934	605	83440	0.70	0.0534	0.0141	0.01235	0.001117	0.0910	0.0247	concordant	79.1	7.2	88.4	24.8
21	1243	63	41442	611	84261	0.70	0.0498	0.0138	0.01178	0.001073	0.0810	0.0230	concordant	75.5	6.9	79.1	23.0
22	3121	161	63536	1499	206646	0.44	0.0509	0.0096	0.01207	0.000960	0.0847	0.0164	concordant	77.3	6.2	82.5	16.5
23	1707	87	63602	818	112745	0.81	0.0502	0.0121	0.01209	0.001041	0.0837	0.0207	concordant	77.5	6.7	81.7	20.8
24	1435	83	46138	656	90444	0.73	0.0574	0.0141	0.01268	0.001124	0.1004	0.0254	concordant	81.2	7.2	97.1	25.5
25	1631	71	55562	768	105858	0.75	0.0430	0.0112	0.01231	0.001067	0.0731	0.0195	concordant	78.9	6.9	71.6	19.6
26	1409	77	49153	716	98748	0.71	0.0540	0.0137	0.01140	0.001014	0.0849	0.0221	concordant	73.1	6.5	82.8	22.2
27 †	1740	68	57962	859	118478	0.70	0.0386	0.0103	0.01173	0.001007	0.0625	0.0169	–22.1	75.2	6.5	61.6	17.1
28	1717	70	66166	824	113667	0.83	0.0403	0.0106	0.01207	0.001038	0.0671	0.0180	concordant	77.3	6.7	65.9	18.1
29	1973	94	89660	926	127742	1.00	0.0471	0.0109	0.01234	0.001039	0.0802	0.0191	concordant	79.1	6.7	78.3	19.2
30	2700	139	106287	1257	173290	0.88	0.0509	0.0101	0.01245	0.001006	0.0874	0.0179	concordant	79.8	6.5	85.1	18.0
Standards																	
GJ1 3-1	20591	1305	6866	1299	179139	0.05	0.0596	0.0090	0.09222	0.005575	0.75898	0.11593	concordant	568.6	35.8	573.4	111.4
GJ1 3-2	20428	1263	6478	1212	167096	0.05	0.0582	0.0088	0.09808	0.005932	0.78750	0.12111	concordant	603.1	38.1	589.8	116.1
PSV 3-1	17905	1093	23033	1966	271013	0.12	0.0574	0.0088	0.05300	0.003214	0.42021	0.06356	concordant	332.9	20.7	356.2	62.6
PSV 3-2	19801	1122	20139	2245	309550	0.09	0.0533	0.0081	0.05132	0.003102	0.37765	0.05669	concordant	322.6	20.0	325.3	56.0
PSV 3-3	20251	1143	20163	2194	302460	0.09	0.0531	0.0081	0.05371	0.003245	0.39374	0.05907	concordant	337.3	20.9	337.1	58.3
OD3 3-1	616	25	67219	670	92327	1.04	0.04010	0.01682	0.00533	0.00057	0.02950	0.01237	concordant	34.3	3.7	29.5	12.5
OD3 3-2	1870	88	265878	2091	288247	1.32	0.04650	0.01110	0.00518	0.00044	0.03326	0.00796	concordant	33.3	2.8	33.2	8.0
OD3 3-3	2363	103	378078	2714	374154	1.44	0.04307	0.00962	0.00505	0.00041	0.02999	0.00672	concordant	32.4	2.7	30.0	6.8
OD3 3-4	2186	115	354104	2636	363416	1.39	0.05198	0.01115	0.00481	0.00040	0.03447	0.00741	concordant	30.9	2.6	34.4	7.5

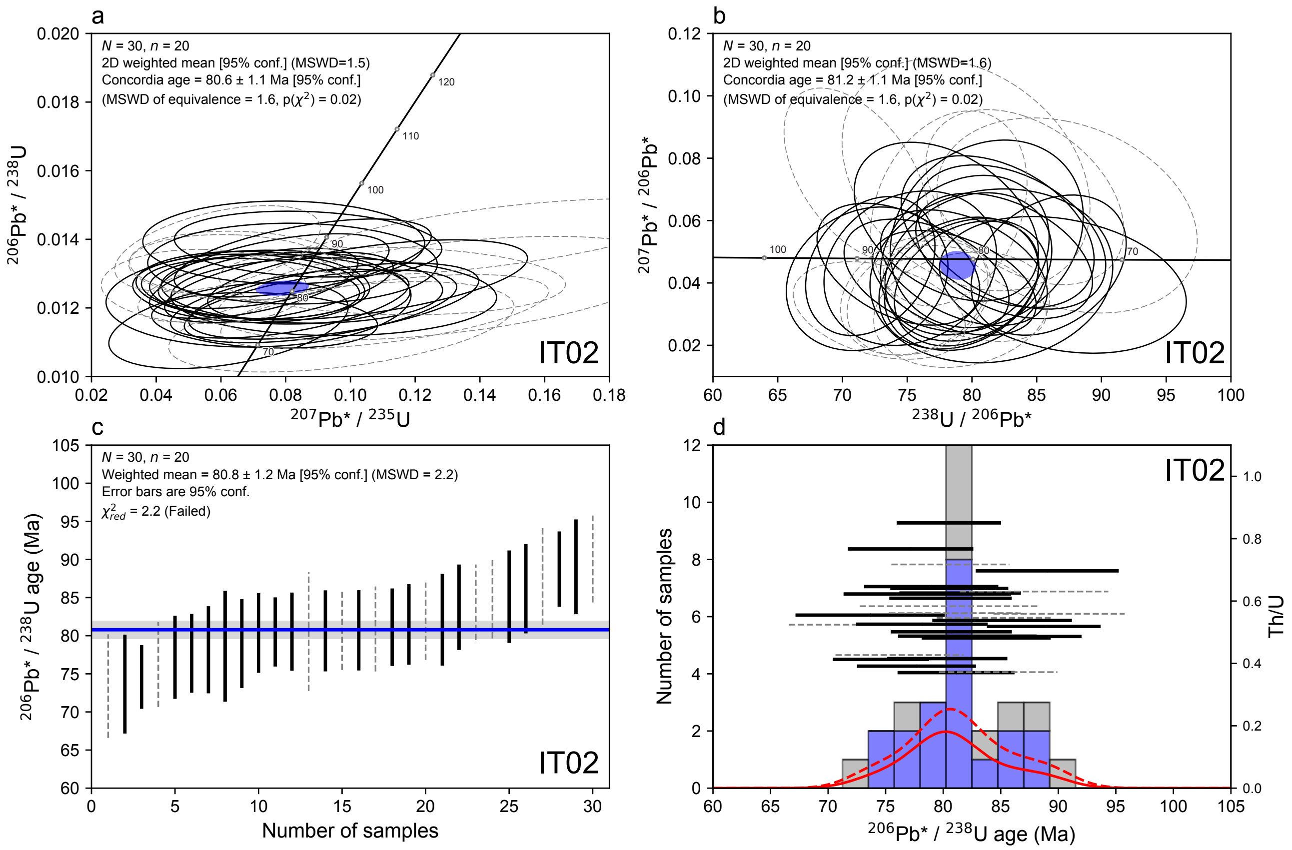

Fig.5 Results of U–Pb dating of IT02. The description is the same as for Fig. 4.

are not identical each other. Therefore, we consider that the tuff beds we analyzed in this study had been obtained from the different sedimentary unit.

Regarding the second interpretation, the Izumi Group in the Ikeda district (the upper Takikubo Formation and the lower Horita Formation) belongs to a single fossil zone, namely, the *Metaplacenticeras subtilistriatum* Ammonite Zone (Bando and Hashimoto, 1984) or the *Archaeodictyomitra lamellicostata* Radiolarian Zone (Hashimoto *et al.*, 2015). The fossil and U–Pb data therefore imply that the period of deposition was so short that the fossil assemblage did not change and the deposition rapidly occurred within the range of uncertainties of the U–Pb ages. An apparent total sediment thickness of 12 km from the lower Takikubo Formation to the lower Horita Formation yields a deposition rate of 3.5 m kyr^{-1}, if this succession had been deposited between 79.3 + 1.1 and 78.3 – 1.3 Ma (Fig. 7). This rate is higher than the depositional rate in the Kazusa Group (2.0–3.0 m kyr^{-1}; Kazaoka *et al.*, 2015) and three times higher than that in the Kumano Basin (1.0–1.3 m kyr^{-1}; Moore *et al.*, 2015). However, this would be possible if intensive igneous flare-up events around ca. 80 Ma (Sato *et al.*, 2016b) provided huge amounts of detritus to the basin of the Izumi Group in a short time period.

The third interpretation is that volcanoes in the hinterland that could have produced new zircon crystals were quiescent during the deposition of this succession. Zircon grains in the tuff beds were sourced from the volcanic rocks that were generated before the deposition of the Takikubo Formation. Most of the reported U–Pb ages from volcanic rocks in the Sanyo Belt in the Chugoku district are older than 80 Ma (Fig. 1); the youngest is 78.9 Ma, from the Ikuno Formation (Sato, 2015). There are no ages younger than 78.9 Ma reported from volcanic rocks except for the Koto Group in the Kinki district (73.5–74.0 Ma; Sato *et al.*, 2016b). Because there is no known volcanic activity between 78 and 74 Ma, it is possible that volcanic activity was intermittent and therefore that supply of new zircon crystals was restricted after 78 Ma. If so, it would be difficult to determine precise depositional ages and sedimentation rates during this period.

6. Conclusions

Zircon U–Pb ages were measured in felsic tuffaceous samples of IT01 (upper Takikubo Formation) and IT02 and IT03 (lower Horita Formation) from the Izumi Group in the Ikeda district, eastern Shikoku. The $^{206}Pb/^{238}U$ ages are 78.3 ± 1.3 Ma (IT01), 80.8 ± 1.2 Ma (IT02), and 79.3 ± 1.1 Ma (IT03). The ages of IT01 and IT03 pass the χ^2_{red} statistical test and therefore indicate the maximum depositional ages of the tuff beds. The ages of IT01 and IT03 overlap the age previously reported from the lower

Table 4 U–Pb data from IT02. Daggers (†) and double daggers (‡) denote discordant data and data excluded from the calculation of concordia and weighted mean ages, respectively. Asterisks (*) of $^{206}Pb^*$ and $^{207}Pb^*$ denote radiogenic.

Sample IT02	Total count						Isotopic ratio						Disc.	Age [Ma]			
Grain#	^{206}Pb	^{207}Pb	^{232}Th	^{235}U	^{238}U	Th/U	$^{207}Pb^*/^{206}Pb^*$	2σ	$^{206}Pb^*/^{238}U$	2σ	$^{207}Pb^*/^{235}U$	2σ	[%]	$^{206}Pb^*/^{238}U$	2σ	$^{207}Pb^*/^{235}U$	2σ
1	532	24	14759	204	28181	0.62	0.0423	0.0224	0.0123	0.0011	0.0716	0.0379	concordant	78.6	7.3	70.2	37.8
2 †	1383	96	33154	510	70294	0.56	0.0639	0.0251	0.0128	0.0008	0.1129	0.0431	24.6	81.9	5.1	108.6	42.8
3 †	1469	57	22569	523	72109	0.37	0.0361	0.0154	0.0132	0.0008	0.0659	0.0275	–30.8	84.8	5.2	64.8	27.5
4	1184	63	31307	443	61125	0.61	0.0489	0.0206	0.0126	0.0008	0.0850	0.0349	concordant	80.6	5.3	82.9	34.9
5	1228	60	22244	462	63654	0.42	0.0451	0.0191	0.0125	0.0008	0.0782	0.0324	concordant	80.4	5.3	76.4	32.3
6	1794	77	66382	673	92788	0.85	0.0398	0.0161	0.0126	0.0007	0.0691	0.0271	concordant	80.5	4.6	67.9	27.2
7	1819	90	35283	737	101574	0.41	0.0457	0.0181	0.0116	0.0007	0.0735	0.0281	concordant	74.6	4.2	72.0	28.1
8 †	1058	36	25717	395	54483	0.56	0.0314	0.0149	0.0126	0.0009	0.0548	0.0255	–49.3	80.9	5.6	54.2	25.6
9 ‡	1028	46	28159	348	48045	0.70	0.0413	0.0185	0.0139	0.0010	0.0794	0.0350	concordant	89.0	6.3	77.6	35.0
10	1349	58	21580	502	69247	0.37	0.0400	0.0170	0.0127	0.0008	0.0699	0.0290	concordant	81.1	5.1	68.6	29.1
11	1294	55	36058	485	66925	0.64	0.0395	0.0170	0.0126	0.0008	0.0686	0.0288	concordant	80.5	5.2	67.3	28.8
12	895	54	25665	342	47205	0.65	0.0557	0.0242	0.0123	0.0009	0.0949	0.0405	concordant	79.0	5.9	92.0	40.3
13	978	47	21627	347	47810	0.54	0.0447	0.0199	0.0133	0.0009	0.0821	0.0360	concordant	85.1	6.1	80.1	35.9
14 ‡	1858	91	38009	632	87148	0.52	0.0454	0.0179	0.0139	0.0008	0.0869	0.0332	concordant	88.7	5.0	84.6	33.2
15 †	1605	61	36384	574	79192	0.55	0.0353	0.0149	0.0132	0.0008	0.0642	0.0263	–33.5	84.4	5.0	63.2	26.4
16 †	1265	43	31731	433	59656	0.63	0.0312	0.0126	0.0137	0.0010	0.0589	0.0256	–51.1	87.9	6.5	58.2	25.6
17	1660	83	32785	580	79908	0.49	0.0460	0.0157	0.0135	0.0009	0.0853	0.0319	concordant	86.2	5.9	83.1	31.9
18	1948	95	42369	726	100155	0.50	0.0449	0.0149	0.0126	0.0008	0.0779	0.0284	concordant	80.7	5.3	76.2	28.4
19	1282	78	30186	494	68065	0.53	0.0565	0.0196	0.0122	0.0009	0.0948	0.0360	concordant	78.2	5.7	92.0	35.9
20 †	2220	179	48193	741	102186	0.56	0.0747	0.0224	0.0141	0.0009	0.1446	0.0486	34.3	90.1	5.7	137.2	48.2
21	1441	85	50144	562	77490	0.77	0.0547	0.0186	0.0120	0.0009	0.0908	0.0338	concordant	77.2	5.5	88.2	33.8
22 †	2168	86	67508	809	111559	0.72	0.0367	0.0124	0.0126	0.0008	0.0635	0.0235	–28.9	80.6	5.2	62.5	23.6
23	2001	87	53768	739	101884	0.63	0.0400	0.0135	0.0127	0.0008	0.0701	0.0259	concordant	81.5	5.3	68.8	26.0
24	1759	81	35407	632	87131	0.48	0.0424	0.0145	0.0131	0.0009	0.0763	0.0287	concordant	83.7	5.6	74.7	28.7
25 †	635	42	15874	260	35898	0.52	0.0616	0.0252	0.0114	0.0011	0.0972	0.0429	22.1	73.4	6.8	94.2	42.7
26	727	31	19187	297	40989	0.55	0.0394	0.0176	0.0115	0.0010	0.0623	0.0297	concordant	73.7	6.5	61.4	29.8
27	1270	82	26392	466	64184	0.49	0.0597	0.0205	0.0128	0.0009	0.1053	0.0397	concordant	82.1	6.1	101.6	39.6
28 †	1282	94	25138	506	69812	0.43	0.0675	0.0226	0.0119	0.0009	0.1106	0.0407	28.4	76.2	5.6	106.5	40.5
29	1798	95	31698	697	96042	0.39	0.0487	0.0162	0.0121	0.0008	0.0812	0.0296	concordant	77.7	5.2	79.3	29.7
30 †	565	46	14333	211	29120	0.58	0.0747	0.0299	0.0126	0.0012	0.1292	0.0566	34.7	80.5	7.8	123.4	55.9
Standards																	
OD3 13-1	856	44	77016	774	106740	0.86	0.0475	0.0191	0.00519	0.00043	0.03397	0.0144608	concordant	33.4	2.8	33.9	14.6

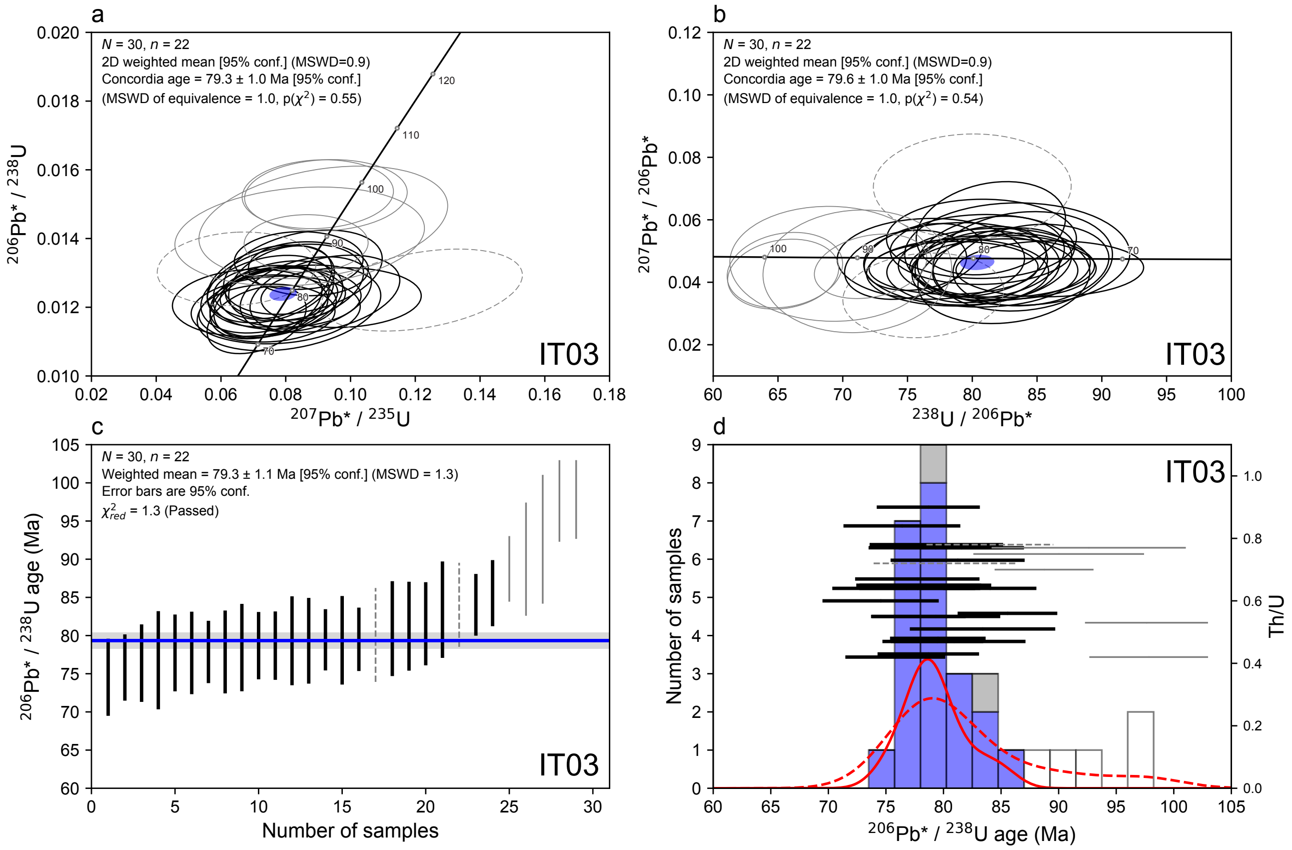

Fig. 6 Results of U–Pb dating of IT03. The description is the same as for Fig. 4. One data point (240.6 Ma) is outside of the plotted region.

Takikubo Formation in the Kan-onji district (KT01: 78.3 ± 0.5 Ma). This suggests that either the deposition occurred over a short period or volcanic activity that produced new zircon crystals in the hinterland (Sanyo Belt) was minimal after 78 Ma.

Acknowledgement

Thin-sections were prepared by Sato Takumi, Owada Akira, Fukuda Kazuyuki and Hirabayashi Eri of the Geoinformation Service Center, National Institute of Advanced Industrial Science and Technology (AIST). This manuscript benefited from thoughtful reviews by Uchino Takayuki. This work is part of study of the quadrangle series, 1:50,000 “Geology of the Ikeda district” conducted by the Geological Survey of Japan, AIST.

Appendix

The generalized ESD (extreme Studentized deviate) test is a common procedure for detecting outliers in data that follow an approximately normal distribution (Rosner, 1983). This test is essentially an iterative application of the Grubbs rejection test (Grubbs, 1950, 1969; Grubbs and Beck, 1972) for eliminating the maximum or minimum outlier. The test statistic for the ith data point is defined as

$$R_i = \frac{\max_i |x_i - \bar{x}|}{\sigma} \qquad \text{(A1)}$$

where $\bar{x}$ is the sample mean and σ is the standard deviation. If the maximum R_i of the ith element is greater than the critical value at a significance level α, then the element is considered to be an outlier. The critical value corresponding to the ith test can be calculated by

$$\lambda_i = \frac{(n-i)t_{p,\nu}}{\sqrt{(n-i+1)(n-i-1+t_{p,\nu}^2)}} \qquad i = 1, 2, \ldots, r$$

where $t_{p,\nu}$ is the $100p$ percentage point from the Student’s t distribution with ν degrees of freedom $(n-i-1)$ and $p = 1 - \alpha / 2(n-i+1)$. The test repeats by increasing i while $R_i > \lambda_i$, and then the number of outliers, r, is determined by finding the largest i from this procedure.

To consider the 2σ uncertainties and the weighted mean, we modify Eq. (A1) to get

$$R_i = \begin{cases} \dfrac{|(x_i - 2\sigma_i) - \mu|}{2\sigma_w} & \text{maximum value, when } (x_i - 2\sigma_i) > \mu \\ \dfrac{|(x_i + 2\sigma_i) - \mu|}{2\sigma_w} & \text{minimum value, when } (x_i + 2\sigma_i) < \mu \end{cases}$$

where μ and σ_w are the weighted sample mean and

Table 5 U–Pb data from IT03. Daggers (†) and double daggers (‡) denote discordant data and data excluded from the calculation of concordia and weighted mean ages, respectively. Asterisks (*) of $^{206}Pb^*$ and $^{207}Pb^*$ denote radiogenic.

Sample IT03	Total count						Isotopic ratio						Disc.	Age [Ma]			
Grain#	^{206}Pb	^{207}Pb	^{232}Th	^{235}U	^{238}U	Th/U	$^{207}Pb^*/^{206}Pb^*$	2σ	$^{206}Pb^*/^{238}U$	2σ	$^{207}Pb^*/^{235}U$	2σ	[%]	$^{206}Pb^*/^{238}U$	2σ	$^{207}Pb^*/^{235}U$	2σ
1	1973	103	39879	951	131132	0.43	0.0481	0.0105	0.01228	0.000688	0.0815	0.0175	concordant	78.7	4.4	79.5	17.7
2	2461	120	55818	1174	161884	0.48	0.0449	0.0092	0.01241	0.000648	0.0769	0.0154	concordant	79.5	4.2	75.2	15.5
3	1842	91	37882	922	127150	0.42	0.0455	0.0105	0.01183	0.000677	0.0742	0.0169	concordant	75.8	4.4	72.7	17.0
4	2760	140	60792	1317	181646	0.47	0.0467	0.0090	0.01240	0.000626	0.0799	0.0149	concordant	79.5	4.0	78.1	15.1
5 ‡	2398	111	37983	929	128028	0.42	0.0426	0.0090	0.01529	0.000806	0.0899	0.0188	concordant	97.8	5.2	87.4	18.9
6	1881	117	79852	907	125023	0.90	0.0573	0.0120	0.01228	0.000699	0.0971	0.0199	concordant	78.7	4.5	94.1	20.0
7 †	1260	49	43700	569	78410	0.78	0.0358	0.0109	0.01312	0.000860	0.0648	0.0197	–31.8	84.0	5.5	63.8	19.8
8 ‡	713	34	22274	300	41400	0.75	0.0435	0.0158	0.01406	0.001158	0.0843	0.0310	concordant	90.0	7.5	82.2	31.0
9 ‡	3212	157	94930	1371	189101	0.70	0.0451	0.0083	0.01386	0.000671	0.0863	0.0154	concordant	88.7	4.3	84.0	15.5
10	2425	120	63913	1182	162941	0.55	0.0457	0.0094	0.01215	0.000637	0.0766	0.0153	concordant	77.8	4.1	74.9	15.4
11	1216	62	49805	604	83224	0.84	0.0467	0.0128	0.01192	0.000792	0.0769	0.0210	concordant	76.4	5.1	75.2	21.1
12	3276	171	93579	1478	203838	0.64	0.0481	0.0086	0.01312	0.000631	0.0870	0.0149	concordant	84.0	4.1	84.7	15.1
13 ‡	2748	136	66475	1217	167868	0.56	0.0456	0.0089	0.01336	0.000676	0.0840	0.0160	concordant	85.6	4.4	81.9	16.1
14 ‡	2120	101	42447	823	113416	0.53	0.0439	0.0097	0.01526	0.000835	0.0924	0.0202	concordant	97.6	5.4	89.7	20.3
15	1304	58	39790	636	87732	0.64	0.0412	0.0116	0.01213	0.000785	0.0690	0.0193	concordant	77.7	5.1	67.7	19.4
16	1179	61	37834	575	79317	0.64	0.0490	0.0132	0.01198	0.001003	0.0810	0.0228	concordant	76.8	6.5	79.1	22.8
17	3218	150	106848	1551	213803	0.67	0.0442	0.0078	0.01213	0.000843	0.0739	0.0139	concordant	77.7	5.4	72.4	14.1
18	1876	94	44702	842	116147	0.51	0.0475	0.0104	0.01302	0.000986	0.0853	0.0197	concordant	83.4	6.4	83.1	19.9
19	2303	111	74161	1100	151677	0.65	0.0457	0.0093	0.01224	0.000893	0.0771	0.0165	concordant	78.4	5.8	75.4	16.7
20 ‡	4594	225	41928	706	97402	0.57	0.0464	0.0069	0.03802	0.002544	0.2434	0.0420	concordant	240.6	16.4	221.2	41.8
21 ‡	860	42	27670	348	47924	0.77	0.0459	0.0148	0.01447	0.001318	0.0916	0.0309	concordant	92.6	8.5	89.0	30.9
22	1741	84	38989	806	111135	0.47	0.0459	0.0106	0.01263	0.000970	0.0799	0.0194	concordant	80.9	6.2	78.1	19.5
23	3136	149	102226	1509	208094	0.65	0.0451	0.0080	0.01215	0.000847	0.0756	0.0143	concordant	77.8	5.5	74.0	14.4
24	2229	102	83888	1053	145119	0.77	0.0435	0.0092	0.01238	0.000909	0.0743	0.0165	concordant	79.3	5.9	72.8	16.6
25 †	1746	130	60917	816	112558	0.72	0.0707	0.0135	0.01250	0.000960	0.1220	0.0250	31.5	80.1	6.2	116.9	25.0
26	2822	150	76465	1332	183696	0.55	0.0505	0.0090	0.01238	0.000876	0.0862	0.0163	concordant	79.3	5.6	84.0	16.5
27	2578	117	89491	1189	163893	0.73	0.0431	0.0086	0.01268	0.000909	0.0754	0.0158	concordant	81.2	5.9	73.8	15.9
28	4554	214	167417	2091	288323	0.77	0.0446	0.0068	0.01273	0.000850	0.0783	0.0128	concordant	81.6	5.5	76.6	13.0
29	2290	130	87690	1081	149005	0.78	0.0539	0.0102	0.01239	0.000905	0.0921	0.0186	concordant	79.4	5.8	89.5	18.7
30	3968	185	123685	1995	275050	0.60	0.0443	0.0072	0.01163	0.000788	0.0710	0.0123	concordant	74.5	5.1	69.6	12.4
Standards																	
GJ1 4-1	21663	1354	7164	1386	191092	0.05	0.05756	0.00586	0.09253	0.00331	0.73496	0.070470	concordant	570.5	21.3	559.5	69.1
GJ1 4-2	21694	1364	7320	1365	188230	0.05	0.05791	0.00589	0.09407	0.00337	0.75164	0.072157	concordant	579.6	21.7	569.2	70.7
PSV 4-1	37419	2087	61260	4030	555686	0.15	0.05137	0.00494	0.05496	0.00190	0.38957	0.030829	concordant	344.9	12.2	334.1	30.8
PSV 4-2	41840	2286	67773	4506	621326	0.15	0.05032	0.00479	0.05496	0.00189	0.38164	0.029539	concordant	344.9	12.2	328.2	29.6
OD3 5-1	1489	80	195963	1826	251768	1.04	0.05113	0.01211	0.00477	0.00038	0.03361	0.008117	concordant	30.7	2.4	33.6	8.2
OD3 5-2	963	36	105586	1099	151575	0.93	0.03508	0.01215	0.00512	0.00045	0.02479	0.008663	–32.5	32.9	2.9	24.9	8.8

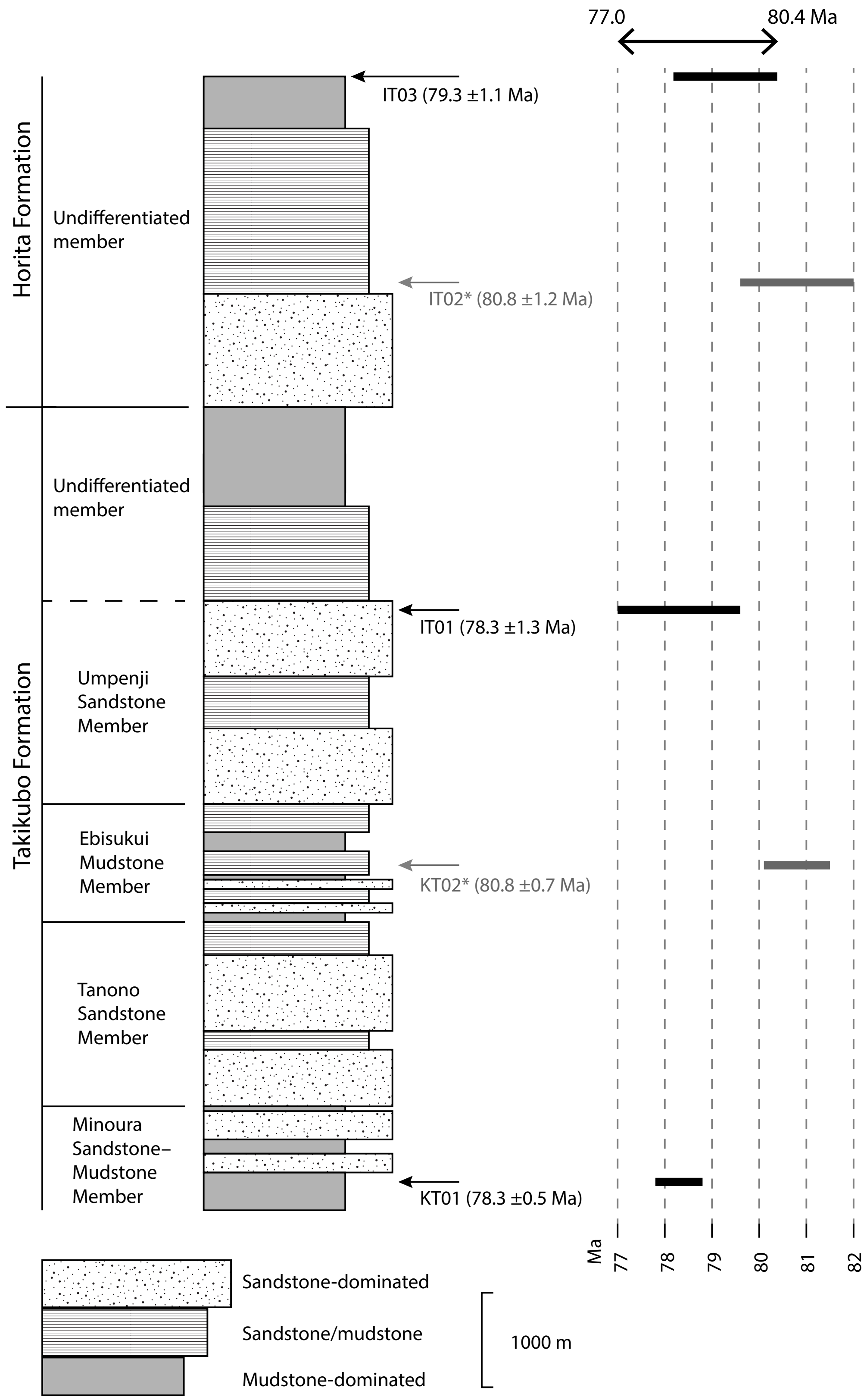

Fig. 7 A generalized stratigraphic column of the main facies from the Kan-onji to Ikeda districts, with the stratigraphic positions of the samples with U–Pb ages. The lithological data are based on Noda *et al.* (2017a) and Matsuura *et al.* (2002). U–Pb ages of KT01 and KT02 come from Noda *et al.* (2017b). Ages with asterisks (*) are rejected data by the χ^2_{red} statistical test (Spencer *et al.*, 2016). Horizontal bars depict 2σ age uncertainties, with black bars and gray bars representing data accepted and rejected by the χ^2_{red} statistical test, respectively.

the standard error, respectively. We used 0.05 for the significance level, α.

References

Bando, Y. and Hashimoto, H. (1984) Biostratigraphy and ammonite fauna of the Izumi Group (Late Cretaceous) in the Asan Mountains. *Mem. Fac. Educ., Kagawa Univ., II*, **34**, 1–16 (in Japanese with English abstract).

Geological Survey of Japan, AIST ed., (2015) Seamless digital geological map of Japan 1:200,000, May 29, 2015 version, Geological Survey of Japan, National Institute of Advanced Industrial Science and Technology. Available from: https://gbank.gsj.jp/seamless/index_en.html [Accessed: 2019-07-29].

Grubbs, F. E. (1950) Sample criteria for testing outlying observations. *Ann. Math. Stat.*, **21**, 27–58.

Grubbs, F. E. (1969) Procedures for detecting outlying observations in samples. *Technometrics*, **11**, 1–21.

Grubbs, F. E. and Beck, G. (1972) Extension of sample sizes and percentage points for significance tests of outlying observations. *Technometrics*, **14**, 847–854.

Hashimoto, H., Motoyama, S., Ishida, K., Terado, T., Morinaga, H., Nakao, K., Morie, T., Kozai, T., Taisei, O., Fukushima, K. and Kawamura, N. (2003) Geology of the Izumi Group and the Median Tectonic Line in the western Tokushima: Mino-cho district. *Comprehensive Research Report of Mino-cho*, Proceedings of Awa Gakkai, no. 49, 1–12 (in Japanese).

Hashimoto, H., Ishida, K., Yamasaki, T., Tsujino, Y. and Kozai, T. (2015) Revised radiolarian zonation of the Upper Cretaceous Izumi inter-arc basin (SW Japan). *Rev. Micropaléontol.*, **58**, 29–50.

Hoskin, P. W. O. and Schaltegger, U. (2003) The composition of zircon and igneous and metamorphic petrogenesis. *Rev. Mineral. Geochem.*, **53**, 27–62.

Ishida, K., Terado, T., Hashimoto, T., Murata, A., Morinaga, H., Nakao, K. and Morimoto, S. (1993) The Izumi Group and the Median Tectonic Line in the western Asan Mountains: Geology and geompormology in the Miyoshi-cho district, Tokushima Prefecture. *Comprehensive Research Report of Miyoshi-cho*, Proceedings of the Local Workshop, no. 39, Awa Gakkai, 1–20 (in Japanese).

Iwano, H., Orihashi, Y., Danhara, T., Hirata, T. and Ogasawara, M. (2012) Evaluation of fission-track and U–Pb double dating method for identical zircon grains: Using homogeneous zircon grains in Kawamoto Granodiorite in Shimane prefecture, Japan. *Jour. Geol. Soc. Japan*, **118**, 365–375 (in Japanese with English abstract).

Iwano, H., Orihashi, Y., Hirata, T., Ogasawara, M., Danhara, T., Horie, K., Hasebe, N., Sueoka, S., Tamura, A., Hayasaka, Y., Katsube, A., Ito, H., Tani, K., Kimura, J.-I., Chang, Q., Kouchi, Y., Haruta, Y. and Yamamoto, K. (2013) An inter-laboratory evaluation of OD-3 zircon for use as a secondary U–Pb dating standard. *Island Arc*, **22**, 382–394.

Jackson, S. E., Pearson, N. J., Griffin, W. L. and Belousova, E. A. (2004) The application of laser ablation-inductively coupled plasma-mass spectrometry to in situ U–Pb zircon geochronology. *Chem. Geol.*, **211**, 47–69.

Kazaoka, O., Suganuma, Y., Okada, M., Kameo, K., Head, M. J., Yoshida, T., Sugaya, M., Kameyama, S., Ogitsu, I., Nirei, H., Aida, N. and Kumai, H. (2015) Stratigraphy of the Kazusa Group, Boso Peninsula: An expanded and highly-resolved marine sedimentary record from the Lower and Middle Pleistocene of central Japan. *Quat. Int.*, **383**, 116–135.

Lukács, R., Harangi, S., Bachmann, O., Guillong, M., Danišík, M., Buret, Y., von Quadt, A., Dunkl, I., Fodor, L., Sliwinski, J., Soós, I. and Szepesi, J. (2015) Zircon geochronology and geochemistry to constrain the youngest eruption events and magma evolution of the Mid-Miocene ignimbrite flare-up in the Pannonian Basin, eastern central Europe. *Contrib. Mineral. Petrol.*, **170**, 52, doi: 10.1007/s00410-015-1206-8.

Matsumoto, T. (1954) The Izumi Belt along the southern border of the Inner Zone of Southwest Japan. *In* The Cretaceous Research Committee ed., *The Cretaceous System in the Japanese Island*, Japanese Society for the Promotion of Scientific Research, Ch. IV, 125–137.

Matsuura, H., Kurimoto, C., Yoshida, F., Saito, Y., Makimoto, H., Toshimitsu, S., Iwaya, T., Komazawa, M. and Hiroshima, T. (2002) *Geological Map of Japan 1:200,000, Okayama and Marugame*. Geological Survey of Japan, AIST.

Miyata, T. (2004) *Geology of the Kokawa district*, Ch. 5, The Upper Cretaceous Izumi Group. Quadrangle Series, 1:50,000, Geological Survey of Japan, AIST, 28–40 (in Japanese).

Moore, G. F., Boston, B. B., Strasser, M., Underwood, M. B. and Ratliff, R. A. (2015) Evolution of tectono-sedimentary systems in the Kumano Basin, Nankai Trough forearc. *Mar. Petrol. Geol.*, **67**, 604–616.

Nakano, M. (1953) On the Izumi Group of the Central part of the Sanuki Mountain-Range, Japan. *Geol. Rep. Hiroshima Univ.*, **3**, 1–13 (in Japanese with English abstract).

Nishimura, T. (1976) Petrography of the Izumi sandstone in the east of the Sanuki Mountain Range, Shikoku, Japan. *Jour. Geol. Soc. Japan*, **82**, 231–240.

Nishiura, M., Yamasaki, T. and Okumura, K. (1993) Sedimentary structure of the Izumi Group developed in the western part of the Asan Range, Shikoku, Japan. *Jour. Sediment. Soc. Japan*, **38**, 33–44 (in Japanese with English abstract).

Noda, A. (2017) A new tool for calculation and visualization of U–Pb age data: UPbplot.py. *Bull. Geol. Surv. Japan*, **68**, 131–140.

Noda, A. and Sato, D. (2018) Submarine slope–fan sedimentation in an ancient forearc related to contemporaneous magmatism: The Upper Cretaceous Izumi Group, southwestern Japan. *Island Arc*, **27**, e12240.

Noda, A. and Toshimitsu, S. (2009) Backward stacking of submarine channel-fan successions controlled by strike-slip faulting: The Izumi Group (Cretaceous), southwest Japan. *Lithosphere*, **1**, 41–59.

Noda, A., Ueki, T., Kawabata, H., Matsuura, H. and Aoya, M. (2017a) *Geology of Kan-onji district*, Quadrangle Series, 1:50,000, Geological Survey of Japan, AIST, 96p. (in Japanese with English abstract).

Noda, A., Danhara, T., Iwano, H. and Hirata, T. (2017b) LA-ICP-MS U–Pb and fission-track ages of felsic tuff beds of the Takikubo Formation, Izumi Group in the Kan-onji district, eastern Shikoku, southwestern Japan. *Bull. Geol. Surv. Japan*, **68**, 119–130.

Ogg, J. G., Hinnov, L. A. and Huang, C. (2012) Ch. 27, Cretaceous. *In* Gradstein, F. M., Ogg, J. G., Schmitz, M. D., and Ogg, G. M. eds., *The Geologic Time Scale*, Elsevier, 793–853.

Rosner, B. (1983) Percentage points for a generalized ESD many-outlier procedure. *Technometrics*, **25**, 165–172.

Sato, D. (2015) U–Pb zircon dating of the Late Cretaceous volcanic rocks from the Ikuno and Mitsuishi mines area, southwest Japan. *Abstract of the Japan Geoscience Union Meeting*, SCG58-P09.

Sato, D. (2016) Zircon U–Pb and fission-track ages of Late Cretaceous volcanic rocks of the Ieshima Islands, southwest Japan. *Japan. Mag. Mineral. Petrol. Sci*., **45**, 53–61 (in Japanese with English abstract).

Sato, D., Yamamoto, T. and Takagi, T. (2016a) *Geology of the Banshu-Ako district*. Quadrangle Series, 1:50,000, Geological Survey of Japan, AIST (in Japanese with English abstract).

Sato, D., Matsuura, H. and Yamamoto, T. (2016b) Timing of the Late Cretaceous ignimbrite flare-up at the eastern margin of the Eurasian Plate: New zircon U–Pb ages from the Aioi–Arima–Koto region of SW Japan. *Jour. Volcanol. Geotherm. Res*., **310**, 89–97.

Seike, K., Iwano, H., Danhara, T. and Hirano, H. (2013) Tectonics of the Ryoke–Izumi belt of the Izumi Mountains, Southwest Japan from thermochronological data. *Jour. Geol. Soc. Japan*, **119**, 759–775 (in Japanese with English abstract).

Sláma, J., Košler, J., Condon, D. J., Crowley, J. L., Gerdes, A., Hanchar, J. M., Horstwood, M. S. A., Morris, G. A., Nasdala, L., Norberg, N., Schaltegger, U., Schoene, B., Tubrett, M. N. and Whitehouse, M. J. (2008) Plešovice zircon —A new natural reference material for U–Pb and Hf isotopic microanalysis. *Chem. Geol*., **249**, 1–35.

Spencer, C. J., Kirkland, C. L. and Taylor, R. J. M. (2016) Strategies towards statistically robust interpretations of in situ U–Pb zircon geochronology. *Geosci. Frontiers*, **7**, 581–589.

Suyari, K. (1966) Studies of the Izumi Group in the Eastern Asan Mountain Rage, Shikoku (I). *Jour. Sci., Coll. Gen. Educ., Univ. Tokushima*, **1**, 9–14 (in Japanese with English abstract).

Suyari, K. (1973) On the lithofacies and the correlation of the Izumi Group of the Asan Mountain Range, Shikoku. *Sci. Rep. Tohoku Univ., 2nd Series, (Geology), Special Volume*, **6**, 489–495 (in Japanese with English abstract).

Suyari, K., Odoi, Y., Kume, Y., Kondo, K., Toake, S., Sobue, K., Terado, T. and Bando, H. (1968) Studies of the Izumi Group in the Eastern Asan Mountain Rage, Shikoku (II). *Jour. Sci., Coll. Gen. Educ., Univ. Tokushima*, **2**, 7–16 (in Japanese with English abstract).

Tanaka, J. (1993) Sedimentation and tectonics in the Cretaceous, strike-slip Izumi basin, Izumi mountains, Japan. *Jour. Geosci., Osaka City Univ*., **36**, 85–107.

Tanaka, J. and Maejima, W. (1995) Fan-delta sedimentation on the basin margin slope of the Cretaceous, strike-slip Izumi Basin, southwestern Japan. *Sediment. Geol*., **98**, 205–213.

Tera, F. and Wasserburg, G. J. (1972) U-Th-Pb systematics in three Apollo 14 basalts and the problem of initial Pb in lunar rocks. *Earth Planet. Sci. Lett*., **14**, 281–304.

Wendt, I. and Carl, C. (1991) The statistical distribution of the mean squared weighted deviation. *Chem. Geol.: Isotope Geosci. Sec*., **86**, 275–285.

Wetherill, G. W. (1956) Discordant uranium-lead ages, I. *Eos, Trans. Am. Geophys. Union*, **37**, 320–326.

Wiedenbeck, M., Allé, P., Corfu, F., Griffin, W. L., Meier, M., Oberli, F., Quadt, A. V., Roddick, J. C. and Spiegel, W. (1995) Three natural zircon standards for U-Th-Pb, Lu-Hf, trace element and REE analyses. *Geostandards Newsletter*, **19**, 1–23.

Yamasaki, T. (1986) Sedimentological study of the Izumi Group in the northern part of Shikoku, Japan. *Sci. Rep. Tohoku Univ., 2nd Series, Geology*, **56**, 43–70.

Yamasaki, T. (1987) Radiolarian assemblages of the Izumi Group in Shikoku and western Awaji Island, Southwest Japan. *Jour. Geol. Soc. Japan*, **93**, 403–417 (in Japanese with English abstract).

Yokoyama, K. and Goto, A. (2000) Petrological study of the Upper Cretaceous sandstones in the Izumi Group, Southwest Japan. *Mem. Natl. Sci. Mus., Tokyo*, **32**, 7–17.

Recieved August 5, 2019
Accepted November 8, 2019

四国東部の池田地域における和泉層群滝久保層と堀田層の珪長質凝灰岩の LA–ICP–MS ジルコン U–Pb 年代

野田　篤・檀原　徹・岩野　英樹・平田　岳史

要　旨

四国東部の池田地域に分布する和泉層群の滝久保層と堀田層の堆積年代を制約するために，挟在する珪長質な凝灰質岩に含まれるジルコン粒子のLA-ICP-MS U–Pb年代を測定した．測定にあたり，滝久保層の上部から1試料（IT01），堀田層の下部から2試料（IT02とIT03）を採取した．測定によって求められた^{206}Pb/^{238}U年代とその誤差（2σ）は，IT01が78.3 ± 1.3 Ma，IT02が80.8 ± 1.2 Ma，IT03が79.3 ± 1.1 Maであったが，このうちの2試料（IT01とIT03）がχ^2_{red}検定に合格した．検定に合格した2試料が示すU–Pb年代は，採取した凝灰岩の堆積年代の下限を規制し，それは中期カンパニアン期（古地磁気年代層序区分のchron C33n）に相当する．これらの年代値は，西隣の観音寺地域から報告されている滝久保層下部の年代値（80.8–78.3 Ma）とほぼ同じであり，滝久保層下部から堀田層下部にかけての見かけの層厚が12 kmに及ぶにもかかわらず，ジルコンのU–Pb年代値は層序的下位から上位にかけて若くなっていく傾向を見せていない．この理由として，和泉層群の当時の堆積速度が非常に大きかったこと，または若いジルコン結晶を生成・供給する火成活動が後背地において一時的に不活発となっていたことが考えられる．